Comparison and Evaluation of Electromagnetic Absorption Characteristics in Realistic Human Head Models of Adult and Children for 900-MHz Mobile Telephones

Jianqing Wang, *Member, IEEE,* and Osamu Fujiwara, *Member, IEEE*

***Abstract*—The controversy on the dosimetry in children's heads for mobile telephones is still inconsistent. Gandhi's group reported a considerable increase of the spatial peak specific absorption rate (SAR) in children's heads, while Kuster's group claimed that there was not a significant difference in the SAR between children and adults. In this paper, based on Japanese children's statistical data on external shapes of heads, we newly developed two kinds of children's models from a Japanese adult head model. Using the children's head models, we calculated the local peak SAR under the same conditions as those previously employed by Gandhi's and Kuster's groups. Compared to the local peak SAR in the adult head model, we found a considerable increase in the children's heads when we fixed the output power of the monopole-type antenna, but no significant differences when we fixed the effective current of the dipole-type antenna. This finding suggests that the contradictory conclusions drawn by the above two groups may be due to the different conditions in their numerical peak SAR calculations.**

***Index Terms*—Children, dosimetry, mobile telephone, specific absorption rate (SAR).**

I. Introduction

CHIDLREN'S use of mobile telephones is growing, while the dosimetric results in children's heads are still inconsistent. In the guidelines for protecting mobile telephone users in various countries, the basic safety limits are defined in terms of the absorbed power per unit mass, or the specific absorption rate (SAR). In the ANSI/IEEE Standard [1], the peak SAR as averaged over any 1 gr of tissue should not exceed 1.6 W/kg, while in the International Commission on Non-Ionizing Radiation Protection (ICNIRP) and Japanese guidelines [2], [3], the peak SAR as averaged over any 10 gr of tissue should not exceed 2 W/kg. In 2001, the U.K. Independent Expert Group on Mobile Phones reported that, on the basis of the evidence currently available, there is no need for the general population to be worried about the use of mobile telephones. The Group recommended, however, that children less than 16 years of age should be discouraged from using mobile telephones since they may absorb more energy from a given telephone than adults do because of their smaller heads, thinner skulls, and higher tissue conductivity [4].

In 1996, Gandhi *et al.* reported a deeper penetration and considerable increase in the local peak SAR in children's heads by using two scaled children's models. An increase of 50% in the 1-gr averaged spatial peak SAR was found in a scaled 5-year-old head model for a quarter-wavelength ($\lambda/4$) monopole antenna mounted on a metal box at 835 MHz [5]. On the other hand, Kuster *et al.* developed two children's head models from magnetic resonance imaging (MRI) data in 1998 and conducted similar calculations. Their results revealed no significant differences in the peak SAR between adults and children for a 0.45λ dipole antenna at 900 MHz, and this conclusion holds also when children are approximated as scaled adults [6]. In 2000, the authors investigated the peak SAR for a $\lambda/4$ monopole antenna with five scaled children's head models [7]. Similarly to Gandhi's results, an increase of the peak SAR in the children's head models was found, although the increased quantity was less than 50%. In 2002, Gandhi *et al.* expanded their previously reported study to two different MRI-based human head models and demonstrated again a 20% higher 1-gr averaged peak SAR at 835 MHz for the scaled children's model [8]. In the same year, however, Guy *et al.* followed Gandhi's previous calculation by using a different MRI-based human head model and claimed that no significant increase was found in the 1-gr averaged peak SAR in the scaled children's models [9]. To elucidate this contradiction among different groups' results, European Cooperation in the Field of Scientific and Technical Research recently began a short-term mission on this subject (COST281).[1]

In general, a child's head is not a simple scale of an adult's head. The developmental changes in the anatomy of various organs follow a quite different course. For example, the brain is formed in the very early stage of life, while the thickness of the cranial bone has a linear growth during the first six years of life. These developmental changes yield various head shapes in different age groups. In this paper, based on Japanese children's statistical database on external shapes of heads, we newly developed 7- and 3-year-old children's head models from a Japanese adult head. For different parts of the head, we employed different scaling factors in order to derive a scaled children's model

Manuscript received February 1, 2002; revised October 29, 2002.

The authors are with the Department of Electrical and Computer Engineering, Nagoya Institute of Technology, Nagoya 466-8555, Japan.

Digital Object Identifier 10.1109/TMTT.2003.808681

[1][Online]. Available: http://www.cost281.org

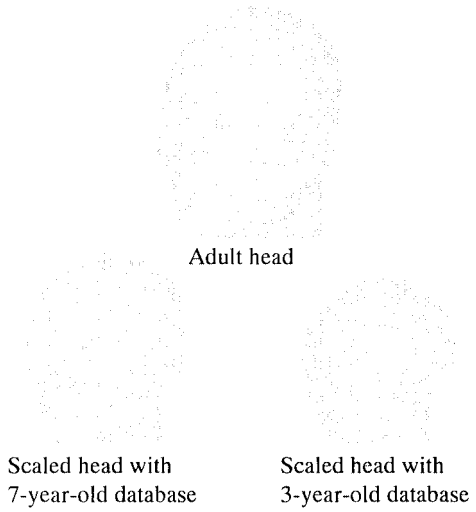

Fig. 1. Head models.

with a more approximated shape to the actual children. Using the two children's head models, we calculated the local peak SAR under almost the same conditions as those previously employed by Gandhi's and Kuster's groups. The results gave a clarification of the contradiction on the dosimetry in children's heads for mobile telephones.

II. Head Models

Fig. 1(a) shows a Japanese adult head model, which was developed in our laboratory based on MRI data [10]. The original raw MRI data were taken from a Japanese adult head (23-year-old male), which consists of 115 slices with a 2-mm space in the axial plane. Each MRI slice had 256×256 pixels and 9-b gray scales. The gray-scale images were segmented unambiguously as belonging to one of 17 different tissue types by assigning each 2-mm cube voxel to a red–green–blue (RGB) code, which identifies the discrete tissue type of that particular voxel. The tissue types are blood, bone, bone marrow, cartilage, cerebrospinal fluid, cornea, dura, fat, gray matter, lens, mucous membrane, muscle, parotid gland, sclera, skin, vitreous humor, and white matter.

Although a scaling down for the adult head is not an accurate representation for a child's head, it is not easy to get MRI data directly for children in general. Accordingly, we developed a scaling procedure to generate the children's head models using different scaling factors for different parts of the head in order to obtain a better approximation to the children. The scaling factors were based on statistical databases on seven parts of the head, i.e., the head length, head breadth, bizygomatic breadth, bigonial breadth, vertex-pupil height, pupil-stomion height, and stomion-gnathion height, as shown in Fig. 2. Table I gives the statistical data and scaling factors for the seven parts, which were cited from Japanese statistical body-size data [11]. In applying the scaling procedure, we kept the resolution to be 2 mm for the two children's head models. We paid special attention to the following two points. First, since the thickness of thin tissues may be less than one cell after the scaling down, we kept at least one cell for these tissues for maintaining the continuity of tissue.

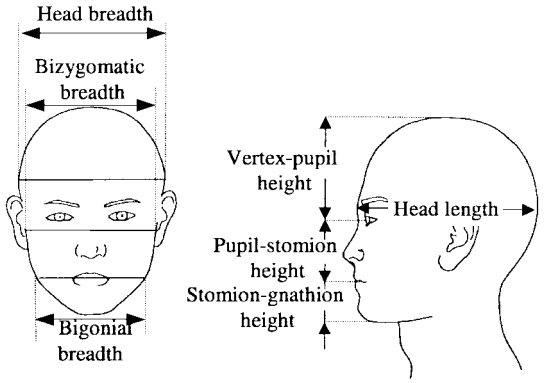

Fig. 2. Measurement parts of head for database.

TABLE I
Statistical Data for Various Parts of Head

	23years old[cm]	7years old[cm]	3years old[cm]
Head length	18.8	17.3(92%)	16.2(86%)
Head breadth	16.0	14.9(93%)	13.9(87%)
Bizygomatic breadth	15.0	13.3(89%)	12.5(83%)
Bigonial breadth	11.6	9.5(82%)	8.8(76%)
Vertex-pupil height	11.5	11.1(97%)	10.5(91%)
Pupil-stomion height	7.5	6.0(80%)	4.2(56%)
Stomion-gnathion height	4.7	3.7(79%)	2.6(55%)

( ): scaling factor

Second, in the vicinity of the boundary of the parts with different scaling factors, we conducted the scaling down according to a gradual change from one scaling factor to another scaling factor for obtaining a smooth head surface. Fig. 1(b) and (c) shows the 7- and 3-year-old head models generated by using the statistical data-based scaling procedure. Comparing them with the adult head shows that the two children's head models are acceptable representations for actual children's heads. Since there are no sufficient data of dielectric properties for children in the literature, we made no distinction between the adult and children. For both the adult and children's models, we, therefore, employed the same dielectric properties of tissues that were derived with the four-cole–cole extrapolation from Gabriel's data [12].

III. Calculation Method

Using the finite-difference time-domain (FDTD) method together with the two newly developed children's head models, we calculated the local peak SAR under almost the same conditions as those previously employed by Gandhi's and Kuster's groups. As shown in Fig. 3(a), being similar to Gandhi's condition, we employed a $\lambda/4$ monopole antenna mounted on a rectangular metal box as a handset of mobile telephone and arranged it in a vertical position. The monopole antenna was mounted on the right-hand-side corner of the metal box, which was in the far end with respect to the side of the earpiece. The earpiece location on the metal box was assumed to be aligned to the center of the auditory canal. Considering that the ear is pressed against the head during the use of a mobile telephone, we partially cut the outer right ears for both the adult and children's head models

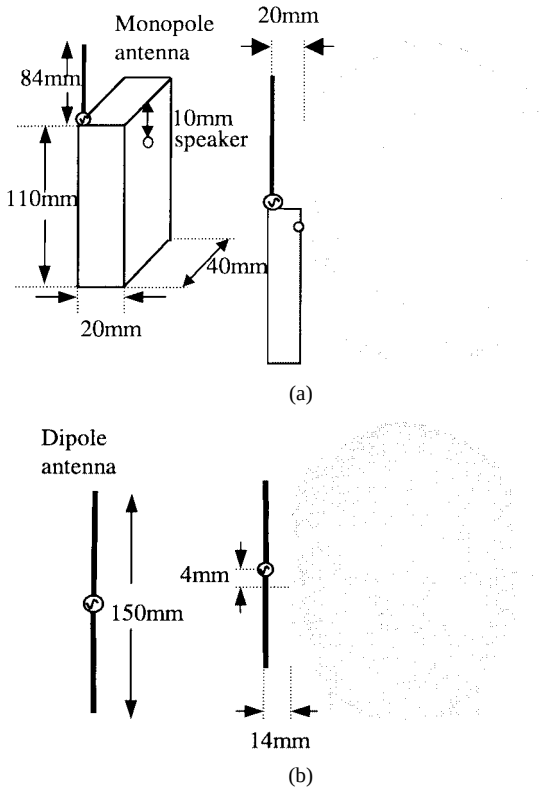

Fig. 3. Configuration of antennas for SAR calculation. (a) $\lambda/4$ monopole antenna mobile telephone. (b) 0.45λ dipole antenna.

and modified them for simulating a pressed situation. As a result, the distance between the monopole antenna and head surface was 2 cm. On the other hand, as shown in Fig. 3(b), being similar to Kuster's condition, we employed a 0.45λ dipole antenna. We arranged the antenna parallel to the body axis and in the plane where the pinna connects to the cheek. Also, we aligned its feeding point so as to have a height of 4 mm higher than the center of the auditory canal. The distance between the antenna and head surface was 1.4 cm. For simulating a pressed situation in this case, we also partially cut the outer right ears for both the adult and children's head models.

It should be emphasized that, under Gandhi's condition, the SAR values were calculated for an antenna output of 0.6 W, while under Kuster's condition, they were given for an effective antenna current of 100 $\mathrm{mA_{rms}}$. It should also be noted that our calculations were not completely identical to Gandhi's or Kuster's conditions. For example, the frequency was 835 MHz in Gandhi's calculation, but 900 MHz in Kuster's and our calculations. In addition, the distance between the antenna and head was 1.5 cm in Kuster's calculation, but 1.4 cm in our calculation.

In our FDTD calculations, we chose the size of cells equal to $2 \times 2 \times 2$ mm. We fed the antenna using a sinusoidal voltage source, and calculated the current flowing through the voltage source cell by integrating the magnetic fields around the voltage source according to Ampere's law. The input impedance of antenna was then derived from the ratio of the voltage and the current together with their phase difference. To absorb the outgoing scattered waves, we employed 12 perfectly matched layers (PMLs) at the boundaries of the calculation domain.

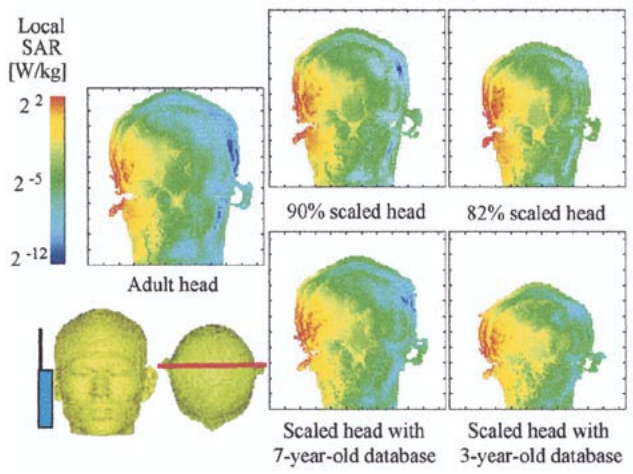

Fig. 4. SAR distributions for the $\lambda/4$ monopole-type antenna with an output power of 0.6 W.

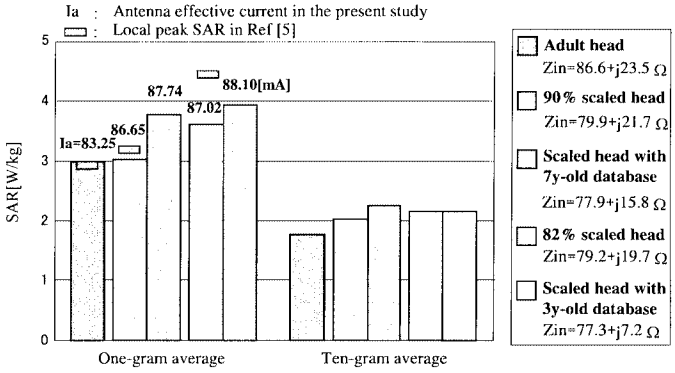

Fig. 5. Local peak SARs for the $\lambda/4$ monopole-type antenna with an output of 0.6 W.

In addition to the 7- and 3-year-old head models based on statistical database, we also calculated the peak SAR for two another head models with fixed scaling factors of 90% and 82%, which corresponds to those of the head circumferences for 7- and 3-year-old children, respectively.

IV. Results and Discussion

Fig. 4 shows the SAR distributions in various head models under Gandhi's condition. For both the adult and children's heads, the maximum SARs were always in the ear region. With penetration into the head, the SAR values decreased rapidly. Compared to the adult head model, however, we observed a deeper penetration in either the children's head models scaled with statistical database or the models scaled with a fixed scaling factor. Fig. 5 shows the 1- and 10-gr averaged spatial peak SARs for the various head models. The 1- and 10-gr averaged spatial peak SARs were derived by shifting a cube of $1 \times 1 \times 1$ cm (1 $\mathrm{cm^3}$) and a cube of $2.2 \times 2.2 \times 2.2$ cm (10.6 $\mathrm{cm^3}$), respectively, across the head volume and computing $\sigma E^2/2\rho$ (σ: conductivity; ρ: tissue density) averaged over the cubes at every position. More than 90% of the space was tissue in the above two cubes. As can be seen from Fig. 5, a considerable increase in the peak SARs was observed in the children's head models. For the 3-year-old head model scaled with the statistical database,

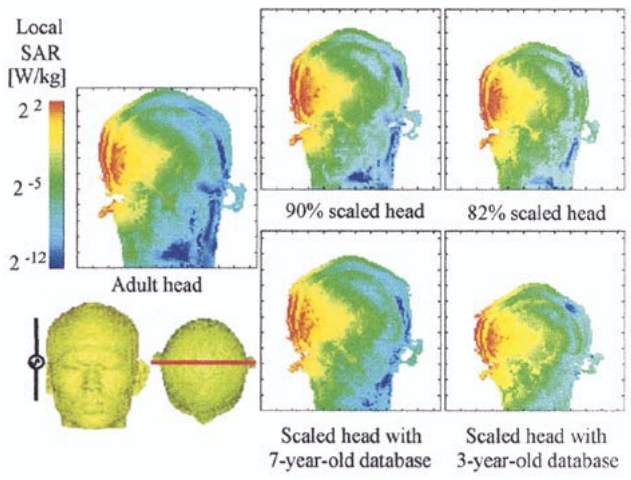

Fig. 6. SAR distributions for the 0.45λ dipole antenna with an effective antenna current of 100 $\mathrm{mA_{rms}}$.

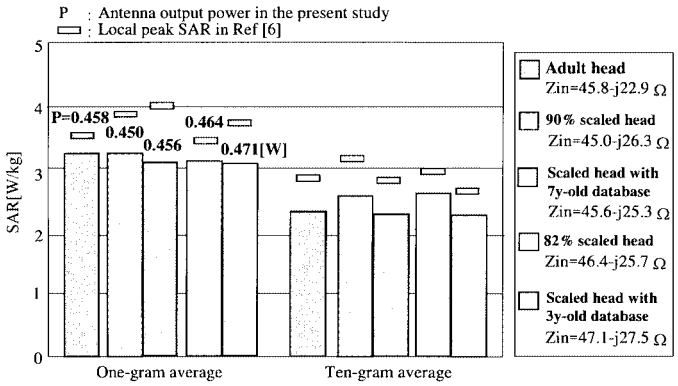

Fig. 7. Local peak SARs for the 0.45λ dipole antenna with an effective antenna current of 100 $\mathrm{mA_{rms}}$.

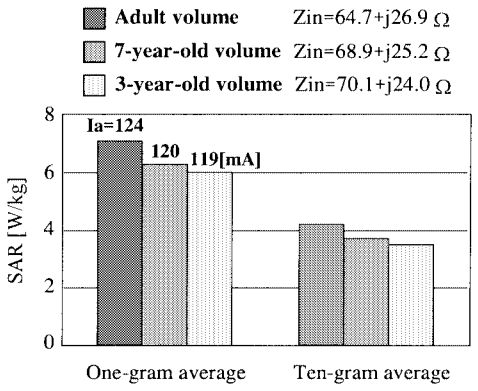

Fig. 8. Local peak SARs for the homogeneous sphere models. The antenna output power was 1 W.

we found an increase of 31.5% in the 1-gr averaged spatial peak SAR and 21.6% in the 10-gr averaged spatial peak SAR compared to the adult head model. For the models scaled with a fixed scaling factor, the increasing trend in the peak SAR also held true. Fig. 5 also depicts with closed bars the 1-gr averaged peak SAR calculated by Gandhi's group for scaled head models. It can be found that our results are very similar to those of Gandhi. Moreover, Fig. 5 gives the effective antenna current Ia and the antenna input impedance $Z\mathrm{in}$. As can be seen in this figure, with the decrease of the head size, the antenna input impedance decreased and, consequently, the antenna current increased because we fixed the antenna output power at 0.6 W. The increase on the antenna current should yield stronger magnetic fields in the vicinity of the antenna. According to the energy absorption mechanism that the SAR in an exposed head is mainly related to the magnetic near field [13], an increased peak SAR in the children's heads is understandable, although the increased quantity on the antenna current is not completely identical to the peak SAR increase.

Fig. 6 shows the SAR distributions in various head models under Kuster's condition. Different from a fixed antenna output power, we fixed the effective antenna current at 100 $\mathrm{mA_{rms}}$. Despite no obvious difference in the in-depth penetration between the adult and 7-year-old heads, some differences between the adult and 3-year-old heads indeed exist. Fig. 7 shows the 1- and 10-gr averaged spatial peak SARs, which demonstrates no significant differences between the adult and children's models. The maximum differences between the adult and children were within 10% for both the 1- and 10-gr averaged spatial peak SARs. These results are similar to Kuster's, which are represented with closed bars in Fig. 7, and support their conclusion. Fig. 7 also gives the antenna output power P and the antenna input impedance $Z\mathrm{in}$. As can be seen in this figure, the variation on the antenna input impedance and, consequently, the antenna output power were insignificant (within 5%) for different head models in this case. The phenomenon of the similar peak SAR levels between the adult and children's heads may attribute to the fixed antenna current and insignificant variation in the input impedance of the 0.45λ dipole antenna.

As a conclusion for the above results, compared to the local peak SAR in the adult head model, we found a considerable increase in the children's heads when we fixed the output power of the monopole-type antenna, but no significant differences when we fixed the effective current of the dipole-type antenna. This finding suggests that the contradictory conclusions drawn by Gandhi's and Kuster's groups are due to the different conditions in their numerical peak SAR calculations.

A worthy point to notice, however, is that the antenna input impedance plays a major role in the peak SAR comparison between the adult and children. In Gandhi's case, the antenna input impedance decreased with decreasing the head sizes and, consequently, the antenna current increased because we fixed the antenna output power. The increase on the antenna current gave an increasing trend for the peak SAR in smaller heads. However, in Kuster's case, the almost constant antenna input impedances and the fixed antenna current gave the insignificant differences in the peak SAR between the adult and children. The third case should be that the antenna input impedance increases with a decrease in the head sizes. To demonstrate this case, we calculated the peak SARs for three different size homogeneous (brain-equivalent tissue) spheres that had the same volumes as the adult, 7-, and 3-year-old head models, respectively. The monopole-type mobile telephone model in Gandhi's case was used in the calculation. Fig. 8 shows the 1- and 10-gr averaged spatial peak SARs, as well as the antenna input impedance and the antenna effective current. It was

found that, with the decrease of the sphere sizes, the resistive components of the antenna input impedance increased and, consequently, the peak SAR decreased because the antenna current decreased for a fixed output power. All of our calculation results, i.e., Gandhi's, Kuster's, and the sphere's cases, can be explained from the variations of the resistive components of the antenna input impedance, although the absolute variation quantity is not identical to the peak SAR.

V. Conclusion

In view of the inconsistent controversy caused by Gandhi's and Kuster's groups on the dosimetry in children's heads for mobile telephones, we did a double check for their calculation results in order to clarity the contradiction. We employed two newly developed children's head models that were scaled with different scaling factors for different parts based on Japanese children's statistical data on external head shapes. Using the children's head models, we calculated the local peak SAR under almost the same conditions as those previously employed by Gandhi's and Kuster's groups. Compared to the local peak SAR in the adult head model, we found an increase of 31.5% in the 1-gr averaged spatial peak SAR and 21.6% in the 10-gr averaged spatial peak SAR in the children's heads when we fixed the output power of the monopole-type antenna, but a differences less than 10% when we fixed the effective current of the dipole-type antenna. This finding suggests that the contradictory conclusions of Gandhi's and Kuster's groups may be due to the different conditions in their numerical SAR evaluations. Moreover, we also showed that all these results can be explained from the variations of the resistive components of the antenna input impedance.

For a real-world mobile telephone, there is not a definitive answer to how the antenna input impedance or the antenna output power varies. It depends on both the system design and power amplifier circuits. If the power amplifier has low output impedance (not acting like a current source), a decrease/increase in the resistive component of the antenna input impedance should increase/decrease the output power and, therefore, the peak SAR. For the case where the mobile telephone has a constant power output, the decrease/increase in the resistive component of the antenna input impedance also increases/decreases the peak SAR. These may be true in most mobile telephones for the Groupe Speciale Mobile (GSM) system. However, in the code division multiple access (CDMA) system, it is known that there is a power control loop for keeping the power arriving at the base-station constant. In this case, the variation on the antenna input impedance might not be so significant for the antenna output power. The less absorbed total power in the smaller heads may yield a decrease of the antenna output, and then the peak SAR. A detailed discussion for the real-world mobile telephones would be a future subject because of their complicated situations. Another subject is to evaluate the temperature rise in children's heads with modeling the blood perfusion effect, which may be more important in the safety evaluation of children.

Acknowledgment

The authors would like to thank this Transactions' Editor-in-Chief, David Rutledge, for his very constructive and helpful comments in revising this paper's manuscript. The authors would also like to thank T. Hisada, Nagoya Institute of Technology, Nagoya, Japan, for his help in the numerical calculations.

References

[1] *Safety Levels With Respect to Exposure to Radio Frequency Electromagnetic Fields, 3 kHz to 300 GHz*, ANSI/IEEE Standard C95.1-1992, 1992.
[2] Int. Commission on Non-Ionizing Radiation Protection, "ICNIRP statement health issues related to the use of hand-held radiotelephones and base transmitters," *Health Phys.*, vol. 70, no. 4, pp. 587–593, Apr. 1996.
[3] "Radio-Radiation Protection Guidelines for Human Exposure to Electromagnetic Fields," Telecommun. Technol. Council for the Ministry of Posts and Telecommun. Japan, Tokyo, Japan, Deliberation 89, 1997.
[4] (2000, Apr.) Mobile phones and health. Independent Expert Group on Mobile Phones. [Online]. Available: http://www.iegmp.org.uk/
[5] O. P. Gandhi, G. Lazzi, and C. M. Furse, "Electromagnetic absorption in the human head and neck for mobile telephones at 835 MHz and 1900 MHz," *IEEE Trans. Microwave Theory Tech.*, vol. 44, pp. 1884–1897, Oct. 1996.
[6] F. Schoenborn, M. Burkhardt, and N. Kuster, "Differences in energy absorption between heads of adults and children in the near field of sources," *Health Phys.*, vol. 74, no. 2, pp. 160–168, Feb. 1998.
[7] O. Fujiwara, T. Joukou, and J. Wang, "Dosimetry analysis and safety evaluation of realistic head models for portable telephones" (in Japanese), *Trans. Inst. Electron. Inf. Commun. Eng. B*, vol. J83-B, no. 5, pp. 720–725, May 2000.
[8] O. P. Gandhi and G. Kang, "Some present problems and a proposed experimental phantom for SAR compliance testing of cellular telephones at 835 MHz and 1900 MHz," *Phys. Med. Biol.*, vol. 47, pp. 1501–1518, 2002.
[9] A. W. Guy, C. K. Chou, and G. Bit-Babik, "FDTD derived SAR distributions in various size human head models exposed to simulated cellular telephone handset transmitting 600 mW at 835 MHz," in *24th Bioelectromagnetics Soc. Annu. Meeting*, Quebec, QC, Canada, June 2002, pp. 7–13.
[10] J. Wang and O. Fujiwara, "Numerical and experimental evaluation of dosimetry in the human head for portable telephones" (in Japanese), *Trans. Inst. Electron. Inf. Commun. Eng. B*, vol. J84-B, no. 1, pp. 1–10, Jan. 2001.
[11] *Japanese Body Size Data*, Res. Inst. of Human Eng. for Quality Life, Tokyo, Japan, 1997.
[12] C. Gabriel, "Compilation of the dielectric properties of body tissues at RF and microwave frequencies," Brooks Air Force Base, San Antonio, TX, Tech. Rep. AL/OE-TR-1996–0037, 1996.
[13] Q. Balzano, O. Garay, and T. J. Manning, "Electromagnetic energy exposure of simulated users of portable cellular telephones," *IEEE Trans. Veh. Technol.*, vol. 44, pp. 390–403, Aug. 1995.

Jianqing Wang (M'99) received the B.E. degree in electronic engineering from the Beijing Institute of Technology, Beijing, China, in 1984, and the M.E. and D.E. degrees in electrical and communication engineering from Tohoku University, Sendai, Japan, in 1988 and 1991, respectively.

He was a Research Associate with Tohoku University and a Research Engineer with the Sophia Systems Company Ltd. prior to joining the Department of Electrical and Computer Engineering, Nagoya Institute of Technology, Nagoya, Japan, in 1997, where he is currently an Associate Professor. His research interests include electromagnetic compatibility, bioelectromagnetics, and digital communications.

Osamu Fujiwara (M'84) received the B.E. degree in electronic engineering from the Nagoya Institute of Technology, Nagoya, Japan, in 1971, and the M.E. and the D.E. degrees in electrical engineering from Nagoya University, Nagoya, Japan, in 1973 and in 1980, respectively.

From 1973 to 1976, he was with the Central Research Laboratory, Hitachi Ltd., Kokubunji, Japan, where he was engaged in research and development of system packaging designs for computers. From 1980 to 1984, he was with the Department of Electrical Engineering, Nagoya University. In 1984, he joined the Department of Electrical and Computer Engineering, Nagoya Institute of Technology, where he is currently a Professor. His research interests include measurement and control of electromagnetic interference due to discharge, bioelectromagnetics, and other related areas of electromagnetic compatibility.

Dr. Fujiwara is a member of the Institute of Electrical, Information and Communication Engineers (IEICE), Japan, and the Institution of Electrical Engineers (IEE), Japan.